Available online at www.sciencedirect.com
ScienceDirect
Journal of Molecular Graphics and Modelling 26 (2007) 319–326
Journal of Molecular Graphics and Modelling
www.elsevier.com/locate/JMGM

Density functional theory study of the inner hydrogen atom transfer in metal-free porphyrins: Meso-substitutional effects

Yuexing Zhang [a], Ping Yao [b], Xue Cai [a], Hui Xu [a], Xianxi Zhang [c,**], Jianzhuang Jiang [a,*]

[a] Department of Chemistry, Shandong University, Jinan 250100, PR China
[b] Department of Physics, Shandong University, Jinan 250100, PR China
[c] School of Chemistry and Chemical Engineering, Liaocheng University, Liaocheng 252059, PR China

Received 2 November 2006; received in revised form 12 December 2006; accepted 12 December 2006
Available online 16 December 2006

Abstract

Density functional theory (DFT) calculations were carried out to study the influence of both electron-withdrawing fluorine and electron-donating amidogen meso-substituents on the inner hydrogen transfer in metal-free porphyrins. Twenty-four stable structures (**1**–**24**) and 21 transition states among the stable structures are fully optimized at the B3LYP/6-31G (d) level, and vibration analyses are carried out to verify the optimized structures. It is found that the acidity of the transferred hydrogen atom, the basicity of the nitrogen atoms of the adjacent pyrrole ring, the distance from the transferred hydrogen atom to the nitrogen atom of the adjacent pyrrole ring, and the electronic nature of meso-substituents in transfer paths, all have significant influences on the potential energy barrier of the inner hydrogen transfer in porphyrins. The different transfer paths of each substituted porphyrin are compared, all the transfer barriers are compared to unsubstituted metal free porphyrin, and the infrared and electronic absorption spectra of some important complexes are described. By placing substituents appropriately, the cis–trans transition energy barrier can be greatly decreased, and the *cis*-porphyrin conformer which can be detected spectroscopically may be significantly stabilized. The present work would shed light on tuning the transition barrier by selecting the most appropriate paths and detecting *cis*-porphyrins experimentally.
© 2006 Elsevier Inc. All rights reserved.

Keywords: Metal-free porphyrins; Inner hydrogen transfer; DFT; Electron-withdrawing substituents; Electron-donating substituents

1. Introduction

Tetrapyrroles have been at the focus of multidisciplinary interest for more than 10 decades [1–3]. Some natural porphyrins and metalloporphyrins are perfect functional dyes due to their fascinating structures [4–6]. Porphyrins play such important roles in vital biological processes, in particular photosynthesis (chlorophyll), oxygen transport (hemoglobin), and oxygen activation (cytochrome) processes, that they have been characterized as ''Pigments of Life'' [5].

It is well-known that the two inner hydrogen atoms of metal-free porphyrin can transfer in a framework of four nitrogen sites, and this process is known as N–H tautomerization. Due to the significant importance in photosynthesis and metal coordination chemistry as well as the potential practical applications, the mechanism of N–H tautomerization in metal-free porphyrins have attracted considerable experimental [7–11] and theoretical [12–19] research interests. It is now generally agreed that the N–H tautomerism of metal-free porphyrins occurs in a stepwise manner, proceeding via transient *cis*-porphyrin intermediates which quickly transfer into the *trans*-tautomers [7,9,11–16]. The physical, chemical, and biological properties of porphyrins and metalloporphyrins can be fine-tuned or dramatically altered by introducing heteroatoms or heteroatom-based groups at the β, meso, or both positions of the macrocycle [20,21]. However the effect of meso-substituents on the N–H tautomerization in metal-free porphyrins is less studied. Thus the main aim of this paper is to clarify how the meso-substituents influence the N–H tautomerization action in meso-substituted porphyrins, and whether the *cis*-porphyrin could be stabilized by introducing electron-withdrawing or electron-donating substituents at the meso positions.

* Corresponding author. Tel.: +86 531 88364088; fax: +86 531 88565211.
** Corresponding author.
E-mail address: jzjiang@sdu.edu.cn (J. Jiang).

1093-3263/$ – see front matter © 2006 Elsevier Inc. All rights reserved.
doi:10.1016/j.jmgm.2006.12.008

In this paper, we studied the influence of both electron-withdrawing and electron-donating meso-substituents on the inner hydrogen transfer in metal-free porphyrins with the help of density functional theory (DFT) calculations. The structures of unsubstituted metal-free porphyrin (**1**), its cis-isomer (**2**), their fluorine and amidogen substituted complexes (**3**–**13** and **14**–**24**), and 21 transition states are fully optimized at the B3LYP/6-31G (d) level. Vibration analyses are also carried out to verify the optimized structures. The different influences of the electron-withdrawing fluorine and electron-donating amidogen substituents on the inner hydrogen transfer in porphyrins are discussed in detail by comparing the four factors.

2. Computational details

DFT method with the Becke-Lee-Young-Parr composite of exchange-correlation functional (B3LYP) as implemented in the Gaussian 03 program [22] was used throughout. In all cases, the 6-31G (d) basis set was used. The Berny algorithm using redundant internal coordinates [23] was employed in energy minimization and the default cutoffs were used throughout. The transition states were detected using QST3 method. The primary input of *cis*-porphyrin was got from the *trans*-porphyrin with D_{2h} symmetry by moving an inner hydrogen atom to one of the nitrogen atom of the adjacent pyrrole ring. The optimized *cis*-porphyrin was planar with C_{2v} symmetry. The primary structures of meso-substituted porphyrins were obtained by introducing electron-withdrawing fluorines and electron-donating amidogens to the meso positions of *trans*-porphyrin and *cis*-porphyrin. The second-order saddles of metal-free porphyrin (**1**) and fluorine-substituted metal-free porphyrin (**3**) were also calculated. The 6-31+G (d, p) basis set was also used to calculate the structures and energies of **1** and **2**. For all the structures, vibrational frequency calculations were carried out to characterize the ground and transition states. All calculations were carried out using the Gaussian 03 program [22] on a IBM P690 system housed at Shandong Province High Performance Computing Centre.

3. Results and discussion

3.1. Energetics

To determine whether meso-substitutes could change the mechanism of the inner hydrogen transfer in metal-free porphyrins from two-stepwise pathway to one-step symmetric pathway, calculations are carried out to search the second-order saddles of the one-stepwise symmetric pathway. As shown in Fig. 1 (for detailed structure parameters see Supplementary data), the second-order saddle structure of metal-free porphyrin (**1**) is 25.8 kcal/mol higher in energy than **1**. However, the transfer barrier of the two-stepwise pathway is only 17 kcal/mol (about 9 kcal/mol lower in energy than that of the one-step symmetric pathway). It indicates that two-stepwise pathway is much more favorable than the concerted pathway in energy as having described by any other researchers for metal-free

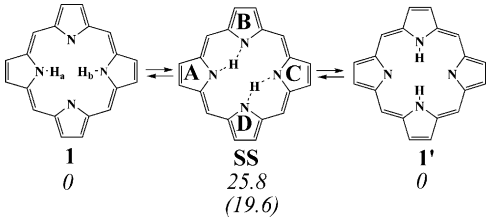

Fig. 1. The calculated structures, energies, and inner hydrogen transfer paths in unsubstituted metal-free porphyrin via the one-stepwise conceterted pathway.

porphyrins [7,9,11–16]. Two different saddles of the concerted inner hydrogen transfer process are found for **3** (Fig. 2). They are both much higher in energy than the transition states of the two-stepwise pathway. This indicates that meso-substitutents can not change the hydrogen transfer mechanism of metal-free porphyrins. Since two-stepwise pathway mechanism has significant advantage in energy compared with the one-stepwise symmetric mechanism according to both the previous and our current studies [7,9,11–16], only two-stepwise pathway mechanism was taken into account in the following discussion of the substitutional effects.

The calculated structures, energies, and inner hydrogen transfer paths of unsubstituted metal-free porphyrins are shown in Fig. 3. The cis-isomer **2** is only 8.4 kcal/mol higher in energy than the trans-isomer **1**, in line with the result of Baker et al. [17] calculated in the same method. Cortina et al. calculated a trans–cis separation of 8.3 kcal/mol with B3LYP/6-31G (d, p) (5D) [24], which is less than our result. When considering the zero-point energy **(ZPE)** corrections, the trans–cis energy difference decreases to 8.1 kcal/mol, which is better than Baker's results with any method. It is noteworthy that upgrading the level of calculation does not reduce the energy difference between **1** and **2** much. For instance, adding a polarization and a diffuse function to the 6-31G (d) basis set only reduces the trans–cis energy difference by about 0.08 kcal/mol. It is noteworthy that the purpose of this paper is to find the most appropriate substituents and transfer path instead of just calculating the exact energy of the complexes. For the reason of time efficiency, only the results obtained from B3LYP/6-31G (d) calculations are used in the following discussion. There are four possible transfer paths in unsubstituted metal-free

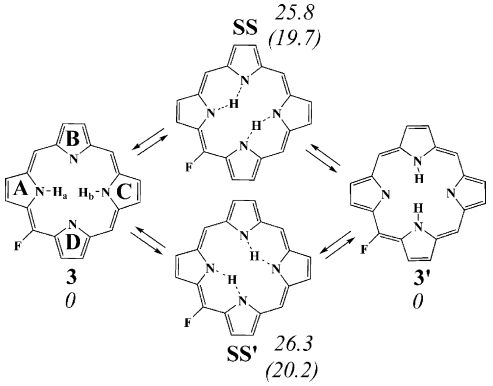

Fig. 2. The calculated structures, energies, and inner hydrogen transfer paths in mono-substituted porphyrins via the one-stepwise conceterted pathway.

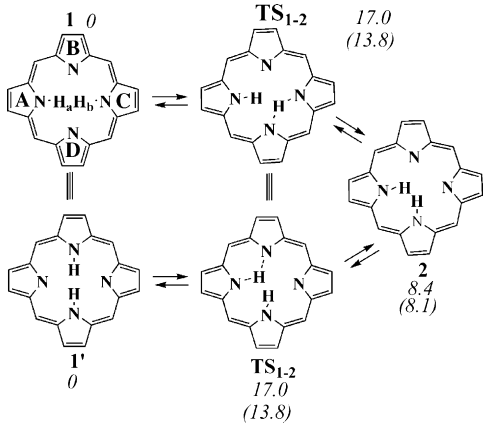

Fig. 3. The calculated structures, energies, and inner hydrogen transfer paths in unsubstituted metal free porphyrins.

porphyrin since the two inner hydrogen atoms, H_a and H_b, can transfer towards both the nitrogen atom of pyrrole rings B and **D** (Fig. 3). Due to the high symmetry of unsubstituted metal-free porphyrin (D_{2h}), the four inner hydrogen transfer paths of unsubstituted metal-free porphyrin are degenerate. The barrier of this transfer path is about 17.0 kcal/mol (13.8 kcal/mol after ZPE correction) according to our calculations, which agrees well with Baker's results.

When one substituent is introduced to the meso position of unsubstituted metal-free porphyrin, the degeneracy of the four inner hydrogen transfer paths disappears. As shown in Fig. 4, the transfer of H_a from the nitrogen atom of pyrrole ring A to B (H_aAB for short) in fluoro-porphyrin (**3**) has a much lower barrier than the other transition paths, and the intermediate of this path, **5**, is more stable than the other cis-isomers. Influenced by the electron-withdrawing fluorine substituent between pyrrole rings A and D, the nitrogen atom of pyrrole ring A (N_A for short) has more negative mulliken charge than C, H_a atom has more positive charge than H_b atom, and the H_a–N_A bond is a little longer than H_b–N_C bond. Thus the acidity of H_a is much stronger than of H_b. Furthermore, N_B (the nitrogen atom of pyrrole ring B) has more affinity to H_a than to H_b due to the shorter distance between H_a and N_B than H_b and N_B. As a result, H_aAB barrier is much lower than H_bCB. Despite the fact that H_a–N_D distance is a little longer than H_b–N_D, the H_aAD barrier is still lower than H_bCD due to the much stronger acidity of H_a than H_b. Since the acidity of H_a is stronger than H_b and the basicity of N_D is stronger than N_B, it seems intricate that the H_aAD barrier is higher than H_bCB. One possible reason is that the electron-withdrawing fluorine substituent joining to the meso carbon atom between A and D makes the meso carbon atom have positive charge, which is disadvantageous to the transfer of H_a. The other reason may be that the distance between H_a and N_D is a little longer than H_b and N_B.

Amidogen substituents have different influence on the inner hydrogen transfer process from fluorine. As shown in Fig. 4 (right), the transfer barrier has the order of H_bCD > H_aAB > H_bCB > H_aAD in energy. The acidity of H_a is also a little stronger than H_b and the basicity of N_D is a little stronger than N_B though amidogen has electron-donating ability instead of the electron-withdrawing property of fluorine. The higher transfer barrier of H_aAB than H_bCB then comes from the longer distance from H_a to N_B than from H_b to N_B. In fact, the distance between H_a and N_B is about 0.2 Å longer than H_b and N_B according to our calculations. As H_a–N_D and H_b–N_B distances are almost equal, the acidity of H and the basicity of N atoms play an important role in influencing the transfer barrier. The stronger acidity of H_a than H_b, the stronger basicity of N_D than N_B, and the advantage of the electron-donating property of the amidogen substituent between A and D to the transition state of H_aAD, together make the barrier of H_aAD a little lower than H_bCB, despite the longer distance between H_a and N_D than H_b and N_B. The same as in fluoro-porphyrins (Fig. 4, left), the

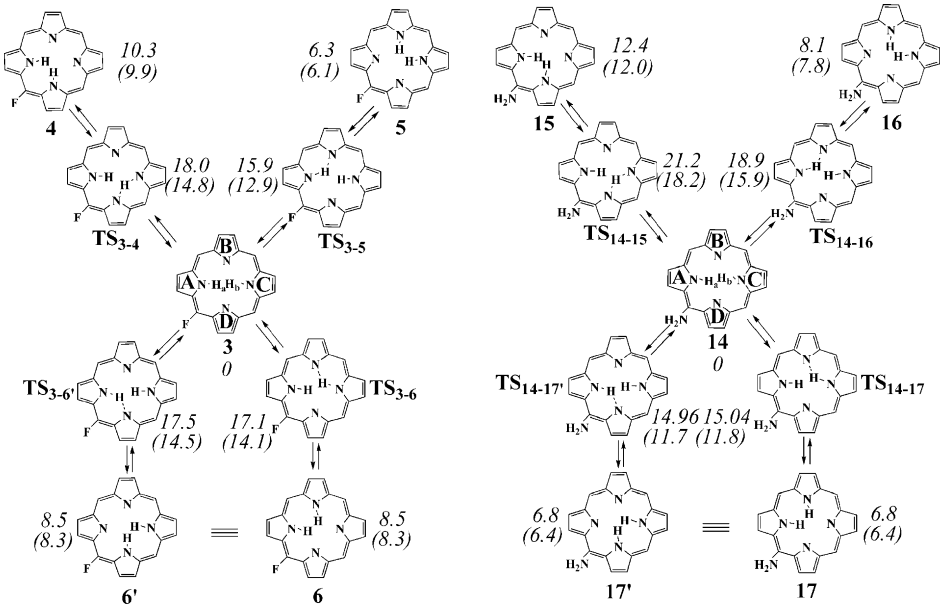

Fig. 4. The calculated structures, energies, and inner hydrogen transfer paths in mono-substituted porphyrins.

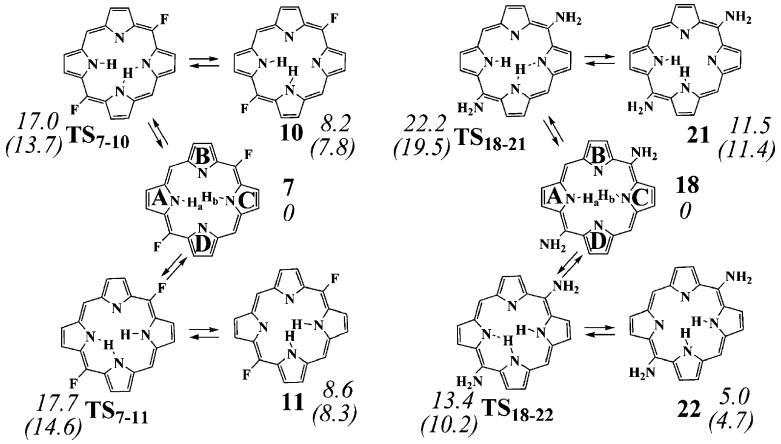

Fig. 5. The calculated structures, energies, and inner hydrogen transfer paths in disubstituted porphyrins with substituents at the para meso positions.

transfer barrier of H_bCD is the highest. This is because the H_b–N_D distance is the longest among all the distances from inner hydrogen atoms to the nitrogen atoms of the adjacent pyrrole ring in **14** (Fig. 4, right).

When two substituents are introduced to the two opposite meso positions of the unsubstituted metal-free porphyrin, only one *trans*-porphyrin (**7** and **18** for fluorine and amidogen substituents, respectively) is obtained. The transfer process of H_aAD is actually equal to H_bCB, and H_aAB equal to H_bCD for **7** due to the C_{2h} symmetry of **7**. Thus only H_aAD and H_bCD processes are discussed here. As H_a–N_D distance is longer than H_b–N_D, and the electron-withdrawing fluorine substituent between A and D is disadvantageous to the transfer of H_a in H_aAD, the barrier of H_aAD is much higher than H_bCD. As for **18** (Fig. 5, right), the environments of H_a and H_b, and N_B and N_D, are still almost equal despite the disappearance of the C_{2h} symmetry. The H_aAD barrier in **18** is 8.8 kcal/mol lower than H_bCD, and it is even about 3.6 kcal/mol lower than the transfer barrier in unsubstituted metal-free porphyrin **1**. This is attributed to such a fact that both the two possible factors influencing the hydrogen transfer are advantageous to the H_aAD process: Firstly, the two amidogens draw the N_A–N_D and N_C–N_B distances near and the N_A–N_B and N_C–N_D distances far, and therefore make the H_a–N_D distance much shorter than H_b–N_D; secondly, the electron-donating substituent between A and D is advantageous to lower the barrier of H_aAD.

As shown in Fig. 6, there are two possible isomers when two fluorines (or amidogens) are introduced to the two meso positions at both sides of the same pyrrole ring (**8** and **9**, or **19** and **20**). For **8** and **19**, H_a and H_b atoms are not equal, but N_B and N_D atoms have the same basicity. On the contrary, the H_a and H_b atoms in **9** and **20** are equal, but N_A and N_C have different environments. As a consequence, only the transfer processes of H_aAD and H_bCD for **8** and **19**, and H_bDA and H_bDC for **9** and **20** are discussed here. Despite the fact that the electron-withdrawing fluorine substituent between A and D is disadvantageous to the hydrogen transfer in H_aAD, and the stronger acidity of H_a than H_b, the closer distance from H_a to N_D than from H_b to N_D in **8** make the transfer barrier of H_aAD about 1.8 kcal/mol lower than H_bCD. As for **9**, the much longer

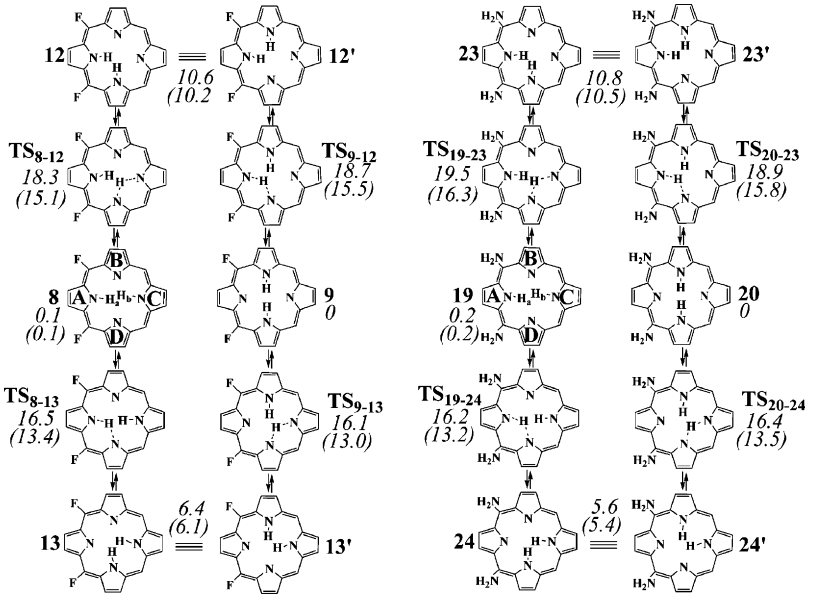

Fig. 6. The calculated structures, energies, and inner hydrogen transfer paths in disubstituted porphyrins with substituents at the adjacent meso positions.

distance between H_b and N_A than N_C, and the disadvantage of the electron-withdrawing fluorine substituent between A and D to the hydrogen transfer in H_bDA, lead to much higher barrier of H_bDA than H_bDC despite the fact that the basicity of N_A is a little stronger than N_C. The weaker acidity of the H_b atom of **8** than the H_b atom of **9**, and the weaker basicity of the N_D atom of **8** than the N_A atom of **9**, would make the H_bCD barrier of **8** higher than the H_bDA barrier of **9**. However, the other two factors, namely the closer distance between H_b and N_D in **8** than between H_b and N_A in **9**, and the disadvantageous influence of the electron-withdrawing fluorine to the H_bDA transfer of **9**, would make the H_bCD barrier of **8** lower than the H_bDA barrier of **9**. The fact that the barrier of H_bCD transfer of **8** is lower than the H_bDA transfer of **9** according to our calculations indicates that the effects of the ''acidity'' and ''basicity'' factors are weaker than the other two factors. It is notable that the intermediate (**12**) obtained by H_bCD transfer of **8** and the intermediate (**12′**) obtained by H_bDA of **9** are actually the same, and they are one of the intermediates from molecule **8** to **9** through inner hydrogen transfer. Similarly, **13** and **13′** are the other intermediates from **8** to **9** through inner hydrogen transfer. As the energy difference between **8** and **9** is only 0.1 kcal/mol, they could exist together and convert to each other through the inner hydrogen transfer. As the energy of the transfer states have the order of H_bDA(**9**) > H_bCD(**8**) > H_aAD(**8**) > H_bDC(**9**), the advantageous inner hydrogen transfer process between **8** and **9** is **8** - H_aAD(**8**)–**13** - H_bDC(**9**)–**9**.

Similar to **8** and **9**, the barrier of H_aAD is lower than H_bCD for **19** due to the stronger acidity of H_a than H_b, the shorter H_a–N_D distance than H_b–N_D, and the advantage coming from the electron-donating amidogen. The barrier of H_bDC is lower than H_bDA for **20** due to the shorter H_b–N_C distance than H_b–N_A, and the stronger basicity of N_C than N_A despite of the advantage coming from the amidogen substituent for H_bDA compared with H_bDC. In contradiction to the transfer paths in **8** and **9**, the H_bDA transfer barrier of **20** is lower than H_bCD of **19** due to the fact that the acidity of H_b in **20** is stronger than the H_b atom of **19**, the H_b–N_A distance in **20** is shorter than the H_b–N_D distance of **19**, and the electron-donating amidogen is favorable to the H_bDA transfer of **20.** As **23** and **23′**, and **24** and **24′** are both the same intermediate structures, the advantageous inner hydrogen transfer process between **19** and **20** is **20** - H_bDC(**20**)–**24** - H_aAD(**19**)–**19** according to the calculated energy order of the transition states, that is, H_bCD(**19**) > H_bDA(**20**) > H_bDC(**20**) > H_aAD(**19**).

The influence of all the meso-substitutes to the inner hydrogen transfer of metal-free porphyrin are summarized in Table 1 according to the four factors as below: (a) the acidity of the transferred inner hydrogen atom; (b) the basicity of the nitrogen atoms of the adjacent pyrrole ring; (c) the distance between the transfer hydrogen atom and the nitrogen atom of the adjacent pyrrole ring; (d) the influence of substituents to the transfer paths in which the hydrogen giving and accepting pyrrole rings are separated by the substituted meso carbon atom. Factor (a) can be presented by the positive charge on hydrogen atom and the N–H bond length, (b) can be presented by the negative charge on the nitrogen atom, (c) can be obtained

Table 1
Summing-up of the influence of meso-substitutes to the inner hydrogen transfer of metal-free porphyrin

Fluoro-porphyrins							Amido-porphyrins											
3 (A-meso-D)			**7** (A-meso-D B-meso-C)				**8**, **9** (B-meso-A-meso-D)				**14** (A-meso-D)			**18** (A-meso-D B-meso-C)			**19**, **20** (B-meso-A-meso-D)		
Paths[a]	abcd[b]	abcd[c]	Paths[a]	abcd[b]	abcd[c]		Paths[a]	abcd[b]	abcd[c]		Paths[a]	abcd[b]	abcd[c]	Paths[a]	abcd[b]	abcd[c]	Paths[a]	abcd[b]	abcd[c]
H_bCD	×√○○		H_aAD	○√××			H_bDA	○√××			H_bCD	×√×○		H_bCD	×√×○		H_bCD	×√×○	
H_aAD	√√××	√○××	***H_bCD***	○√√○	○○√√		H_bCD	×√×○	××√√		H_aAB	○√×○	√×√○	***H_aAD***	×√√√	○○√√	H_bDA	×√×√	√×√√
H_bCB	×√×○	××√√					***H_aAD***	√√√×	√○√×		***H_bCB***	×√√○	×○√○				***H_bDC***	×√×○	○√√×
H_aAB	√√√○	√○√○					***H_bDC***	○√√○	××√√		***H_aAD***	○√√√	√√×√				***H_aAD***	×√×√	××××√

A–D, the pyrrole ring according to Figs. 1–6; a, acidity of the transfer inner hydrogen atom; b, basicity of the pyrrole ring nitrogen atom accepting the transfer hydrogen atom; c, the distance between the transfer hydrogen and the pyrrole ring nitrogen accepting the transfer hydrogen; d, the influence of the meso-substitute to the hydrogen transfer; √, advantageous to lower the transfer barrier; ×, disadvantageous to lower the transfer barrier; ○, having no influence.

[a] Transfer energy decreasing from top to bottom.

[b] Results comparing to unsubstituted metal-free porphyrin (**1**).

[c] Results comparing to the transfer paths with higher barrier in the same *trans*-porphyrins (comparing to the paths above it).

in the fully optimized structures, and (d) can be determined by the property of the substituents. Electron-withdrawing substituent is disadvantageous to the transfer path described in factor (d), and electron-donating substituent is advantageous to it. The different transfer paths in each substituted porphyrins are compared and listed in energy descending sequence in Table 1, and all the transfer paths barriers are compared to that of unsubstituted metal-free porphyrin with the advantageous paths emphasized in italic and bold face in Table 1. It can be seen that only the transfer paths with two more advantages from the four factors can have barriers lower than in unsubstituted metal-free porphyrin. The exception of H_bDC of **20** may be due to the lengthening of the H_b–N_C distance derived from the non-planar distortion of the macrocycle ring comparing to **1**. It is worth noting that the cis structures obtained in substituted porphyrins with transfer barriers lower than unsubstituted metal-free porphyrin are all more stable than **2**.

3.2. Infrared spectra predictions

As UV/vis and infrared spectra are most promising route to detect *cis*-porphyrin [17], the IR spectra of both the *trans*-porphyrin and *cis*-porphyrin are calculated and the simulated spectra are shown in Fig. 7. Comparing the IR spectra of *trans*-porphyrin and *cis*-porphyrin shown in Fig. 7a, one can easily observe the strong peak at 3245 cm^{-1} of *cis*-porphyrin which is identified as N–H symmetry stretching. This peak does not exist in the spectra of *trans*-porphyrin, and thus can be used as ‘‘fingerprints’’ to detect the presence of *cis*-porphyrin. Even for the mixture of 99% *trans*-porphyrin and 1% *cis*-porphyrin, the peak at 3245 cm^{-1} is still visible, as is shown in Fig. 7a. The N–D symmetry stretching peak in *cis*-*N*′,*N*-dideutetio porphyrin moves to 2388 cm^{-1}, when the two inner hydrogens are changed to deuteriums. As shown in Fig. 7b, the peak at 2388 cm^{-1} which only exists in *cis*-porphyrin-D2 and is also visible even in the mixture with 1% cis-isomers, can be used as fingerprints of *cis*-porphyrin-D2.

Table S4 (Supplementary data) lists the N–H stretching frequencies of *trans*-porphyrins and *cis*-porphyrins, and the vibrational models including inner hydrogen atoms in the transition states. Noting that the N–H symmetry stretching vibrational models in *trans*-porphyrins are very weak and some are not IR active due to the high symmetry of *trans*-porphyrins. As a result, only the N–H asymmetry stretchings of *trans*-porphyrins are given in Table S4 (Supplementary data). Contrary to *trans*-porphyrins, the N–H symmetry stretchings of *cis*-porphyrins result in great changes of the molecular dipole moment and thus give strong intensity vibrations. Much interestingly, there are no other vibrations in *trans*-porphyrins near the N–H symmetry stretching frequencies. Therefore, the N–H symmetry stretching peaks can work as fingerprints to determine the existence of *cis*-porphyrins even in substitutional porphyrins.

As to the frequencies of the transition states, they can give much more information besides verifying the transition states. As the imaginary frequency for every transition state corresponds to the vibrational model pointing to the reactant and product, a smallest frequency should correspond to the easiest transfer process between the transition state and the reactant. As mentioned above, $TS_{18–22}$ has the smallest energy gap to the corresponding *trans*-porphyrin among all the transition states. The frequency calculations also show that $TS_{18–22}$ has the smallest imaginary frequency of all the transition states. This great consistency shows that the calculated energies and frequencies can be used to verify each other. The calculated imaginary frequency for the reaction coordinate in $TS_{1–2}$ (at 1535i cm^{-1} after scale with the factor of 0.9614 [25]), falls in the range obtained from modeling the experimental tautomerization rates by Butenhoff and Moore [7] using the lower value for the pre-exponential factor (5×10^{12}), between 1425i and 1853i cm^{-1}. It consists well with Baker's imaginary frequency at 1583i cm^{-1}(without scaled) [17]. As the N–H stretching frequency has direct relation to the N–H bond length, the calculated N–H stretching frequency can be used to distinguish

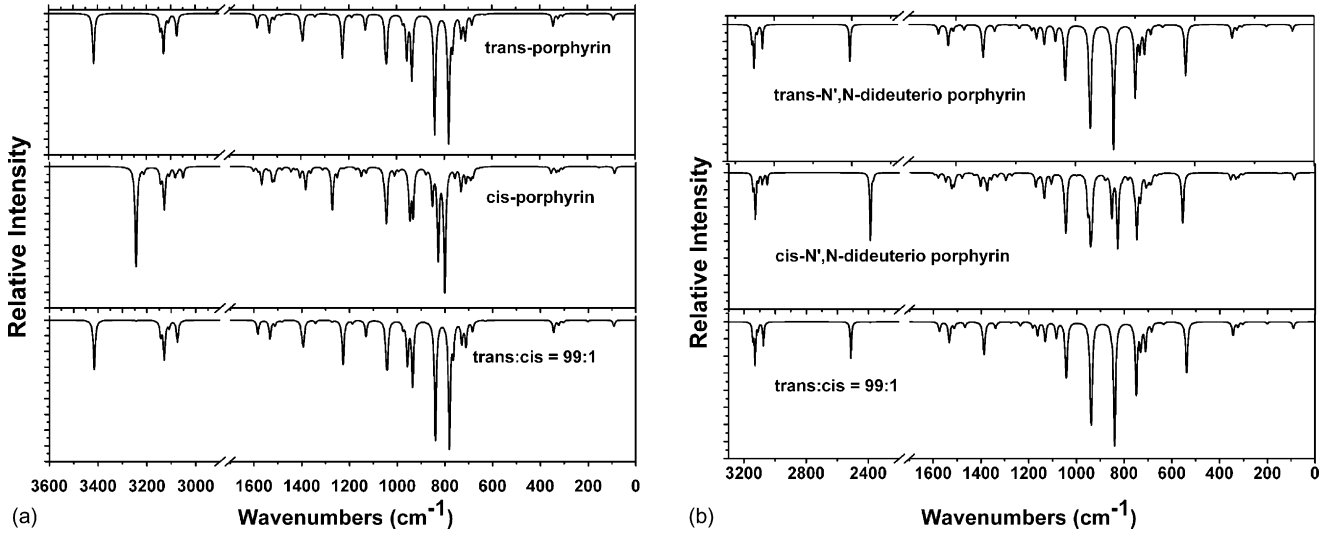

Fig. 7. The simulated IR spectra of metal-free porphyrins. (a) *trans*-Porphyrin and *cis*-porphyrin; (b) *trans*–*N*′,*N*-dideuterio porphyrin and *cis*-*N*′,*N*-dideuterio porphyrin.

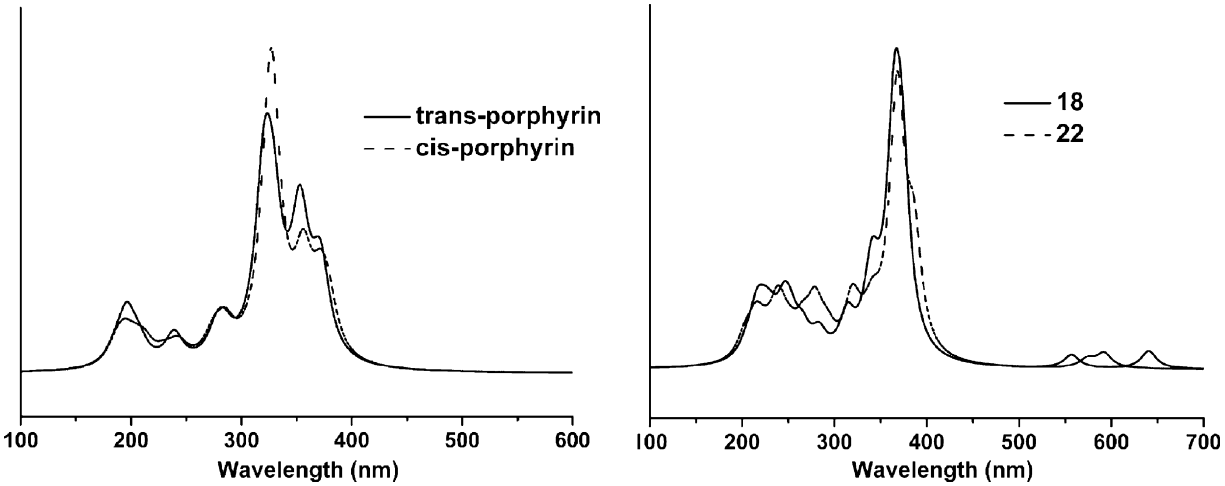

Fig. 8. The simulated UV–vis spectra of (a) *trans*-porphyrin and *cis*-porphyrin, and (b) diamido-porphyrins.

the small difference of the N–H bond length. For example, TS_{3-4} and TS_{9-12} have the similar and longest N_1–H_{25} bond lengths of 1.028 Å, but the N_1–H_{25} stretching frequency of TS_{3-4} is about 5 cm^{-1} smaller than TS_{9-12}, indicating the N_1–H_{25} bond of TS_{3-4} is a few longer than TS_{9-12}. TS_{9-13}, TS_{14-16}, TS_{18-21}, and TS_{19-24} all have similar and shortest N_1–H_{25} bond lengths of 1.023 Å, there corresponding N–H stretching frequencies are among the biggest frequencies but with difference from 0 to 9 cm^{-1}. Other noticeable vibrational modes are the frequencies assigned as *d* in Table S4. They are peculiar in transition states, in which the transitional H atoms vibrate between the meso carbon atoms and the mean centers of the porphyrin macrocycles. Whether the meso carbon atoms are joined by substituents or not, and what kind of substituents they are joined, may have some influences to these frequencies. As the transitional hydrogen atoms have actions with both the two near pyrrole nitrogen atoms, these frequencies are also influenced by the distances between this transitional hydrogen atom and the two neighbor pyrrole nitrogen atoms.

3.3. UV–vis spectra

Fig. 8a shows the simulated absorption spectra of **1** and **2**. Both the *trans*-porphyrin and the *cis*-porphyrin have six absorption peaks. All the peaks except for the two at 284 and 321 nm of *trans*-porphyrin are more intense than that of *cis*-porphyrin due to the larger oscillator strength according to the calculation. As an exception, only the peak at 196 nm of **1** is at the red side of **2**, indicating the energy difference of the orbitals corresponding to this transition of the former is smaller than the latter. This peak is mainly due to the electron transition from HOMO to LUMO + 4 for both **1** and **2** according to the calculation. The HOMO energies of **1** and **2** are equal, but the LUMO + 4 energy of **1** is lower than that of **2**, so the peak of **1** is at the red side of **2**. As the most intense peaks, the peaks at 321 and 326 nm for **1** and **2**, respectively, are mainly due to the electron transition from HOMO − 3 to LUMO or the near degenerate LUMO + 1. Furthermore, this peak of **2** has the largest red shift comparing to that of **1**, and the difference of their intensity is the largest, so this peak can be used to detect the existence of *cis*-porphyrin.

The absorption spectra of **18** and **22**, which have the smallest cis–trans energy difference of the porphyrins studied in this work, are shown in Fig. 8b. There are two more peaks in **18** and **22** than in **1** and **2**, which are in the region from 550 to 650 nm. The weak peaks at 640 nm for **18** and 592 nm for **22** are mainly due to electron transition from HOMO to LUMO according to the calculation, and thus can be attributed to Q bands though the LUMO and LUMO + 1 are not degenerate. As the most intense peaks, the peaks at 365 and 368 nm for **18** and **22** are not well separated as for **1** and **2** due to their near position and intensities. They are mainly due to electron transition from HOMO − 1 to LUMO + 1 and LUMO, respectively. The possible peaks that can be used to detect *cis*-porphyrin are the peaks at 278 nm for **22**, which shifts more than 5 nm to the blue side comparing to **18** and the intensity increases markedly.

4. Conclusion

On the basis of the density functional theory (DFT) calculations of 24 stable structures (**1**–**24**) and 21 transition states, the influence of meso-substituents on the inner hydrogen transfer in metal-free porphyrins is carried out. Considering all the four factors described in the present work, which comes from the reorganization of the macrocycle electrons due to the influence of the meso-substituents, one can rationalize the energies of the various transition states and intermediates of the stepwise tautomerism. The cis–trans energy difference and transition energy barrier during the hydrogen transfer process for free base porphyrin can be reduced 0.15 and 0.16 eV, respectively, by selecting the appropriate meso-substituents. It is concluded that meso-substituents, whether electron-donating or electron-withdrawing, tend to facilitate tautomerization by lowering the barrier along one of the trans–cis–trans path though the effect is small and tends to saturate quickly for multiple substituents. The IR and UV–vis spectra of *cis*-porphyrins have significant differences from the *trans*-porphyrins, and some

characteristic peak can be used as fingerprints to detect *cis*-porphyrins.

Acknowledgements

Financial support from the Natural Science Foundation of China (Grant No. 20325105, 20431010, 20501011), National Ministry of Science and Technology of China (Grant No. 2001CB6105-07), and Ministry of Education of China, Shandong University is gratefully acknowledged. We are also grateful to the Shandong Province High Performance Computing Centre for a grant of computer time.

Appendix A. Supplementary data

The calculated structural parameters and energies of all the stable structures, the calculated energies of the transition states, and the calculated frequencies of the stable structures and transition states. These supplementary data associated with this article can be found, in the online version, at doi:10.1016/j.jmgm.2006.12.008.

References

[1] T. Mashiko, D. Dolphin, Porphyrins, hydroporphyrins, azaporphyrins, phthalocyanines, corroles, corrins and related macrocycles, in: G. Wilkinson (Chief Ed.), Comprehensive Coordination Chemistry, vol. 2, Pergamon, Oxford, 1987, p. 813 (Chapter 21.1).
[2] K.M. Smith, Porphyrins, corrins and phthalo-cyanines, in: A.R. Katritzky, C.W. Rees (Eds.), Comprehensive Heterocyclic Chemistry, vol. 4, Pergamon, Oxford, 1984 , p. 377 (Chapter 3.07).
[3] D. Dolphin (Ed.), The Porphyrins, vols. 1–7, Academic, New York, 1978.
[4] K. Smith (Ed.), Porphyrins and Metalloporphyrins, Elsevier, Amsterdam, 1975.
[5] A.R. Battersby, C.J.R. Fookes, G.W.J. Matcham, E. McDonald, Biosynthesis of the pigments of life: formation of the macrocycle, Nature (London) 285 (1980) 17–21.
[6] B. Kräutler, The porphinoids-versatile biological catalyst molecules, Chimia 41 (1987) 277–292.
[7] T.J. Butenhoff, C.B. Moore, Hydrogen atom tunneling in the thermal tautomerism of porphine imbedded in a *n*-hexane matrix, J. Am. Chem. Soc. 110 (1988) 8336–8341.
[8] M. Schlabach, H. Rumpel, H.-H. Limbach, investigation of the tautomerism of 15N-labeled hydroporphyrins by dynamic NMR spectroscopy, Angew. Chem. Int. Ed. Engl. 28 (1) (1989) 76–79.
[9] T.J. Butenhoff, R.S. Chuck, H.-H. Limbach, C.B. Moore, Vibrational photochemistry of porphine imbedded in a hexane-d14 Shpol'skii matrix, J. Phys. Chem. 94 (20) (1990) 7847–7851.
[10] M. Schlabach, H.-H. Limbach, E. Bunnenberg, A.Y.L. Shu, B.R. Tolf, C. Djerassi, NMR study of kinetic HH/HD/DH/DD isotope effects on the tautomerism of acetylporphyrin: evidence for a stepwise double proton transfer, J. Am. Chem. Soc. 115 (11) (1993) 4554–4565.
[11] J. Braun, M. Schlabach, B. Wehrle, M. Köcher, E. Vogel, H.-H. Limbach, NMR study of the tautomerism of porphyrin including the kinetic HH/HD/DD isotope effects in the liquid and the solid state, J. Am. Chem. Soc. 116 (15) (1994) 6593–6604.
[12] V.A. Kuzmitsky, K.N. Solovyov, Quantum-chemical study of nh tautomerism in porphin, J. Mol. Struct. 65 (1980) 219–230.
[13] A. Sarai, Dynamics of proton migration in free base porphines, J. Chem. Phys. 76 (11) (1982) 5554–5563.
[14] A. Sarai, Comment on "IR-spectroscopic study of isotope effects on the NH/ND stretching bands of meso-tetraphenylporphine and vibrational hydrogen tunneling", J. Chem. Phys. 80 (10) (1984) 5341–5343.
[15] K.M.J. Merz, C.H. Reynolds, Tautomerism in free base porphyrins: the porphyrin potential energy surface, J. Chem. Soc. Chem. Commun. (1988) 90–92.
[16] Z. Smedarchina, W. Siebrand, F. Zerbetto, Comparison of synchronous and asynchronous hydrogen transfer mechanisms in free-base porphyrins, Chem. Phys. 136 (2) (1989) 285–295.
[17] J. Baker, P.M. Kozlowski, A.A. Jarzecki, P. Pulay, The inner-hydrogen migration in free base porphyrin, Theor. Chem. Acc. 97 (1997) 59–66.
[18] Z. Smedarchina, M.Z. Zgierski, W. Siebrand, P.M. Kozlowski, Dynamics of tautomerism in porphine: an instanton approach, J. Chem. Phys. 109 (3) (1998) 1014–1024.
[19] D.K. Maity, R.L. Bell, T.N. Truong, Mechanism and quantum mechanical tunneling effects on inner hydrogen atom transfer in free base porphyrin: a direct ab initio dynamics study, J. Am. Chem. Soc. 122 (5) (2000) 897–906.
[20] P.G. Gassman, A. Ghosh, J. Almlöf, Electronic effects of peripheral substituents in porphyrins: X-ray photoelectron spectroscopy and ab initio self-consistent field calculations, J. Am. Chem. Soc. 114 (25) (1992) 9990–10000.
[21] A. Ghosh, Ab initio Hartree-Fock and local density functional calculations on prototype halogenated porphyrins. Do electrochemically measured substituent effects reflect gas-phase trends, J. Phys. Chem. 98 (1994) 11004–11006.
[22] M.J. Frisch, et al., Gaussian 03, Revision B05, Gaussian, Inc., Wallingford, CT, 2004.
[23] C. Peng, P.Y. Ayala, H.B. Schlegel, M.J. Frisch, Using redundant internal coordinates to optimize equilibrium geometries and transition states, J. Comp. Chem. 17 (1) (1996) 49–56.
[24] H. Cortina, M.L. Senent, Y.G. Smeyers, Ab initio comparative study of the structure and properties of H2-porphin and H2-phthalocyanine. The electronic absorption spectra, J. Phys. Chem. A 107 (42) (2003) 8968–8974.
[25] R.D. Johnson III (Ed.), NIST Computational Chemistry Comparison and Benchmark Database, NIST Standard Reference Database Number 101 Release 10, May 2004, http://srdata.nist.gov/cccbdb.